University of Reading

Intensified impact of tropical Atlantic SST on the western North Pacific summer climate under a weakened Atlantic thermohaline circulation

Article

Accepted Version

Chen, W., Lee, J.-Y., Lu, R., Dong, B. ORCID: https://orcid.org/0000-0003-0809-7911 and Ha, K.-J. (2015) Intensified impact of tropical Atlantic SST on the western North Pacific summer climate under a weakened Atlantic thermohaline circulation. Climate Dynamics, 45 (7-8). pp. 2033-2046. ISSN 1432-0894 doi: 10.1007/s00382-014-2454-4 Available at https://centaur.reading.ac.uk/40528/

It is advisable to refer to the publisher's version if you intend to cite from the work. See Guidance on citing.
Published version at: http://link.springer.com/article/10.1007%2Fs00382-014-2454-4
To link to this article DOI: http://dx.doi.org/10.1007/s00382-014-2454-4

Publisher: Springer

All outputs in CentAUR are protected by Intellectual Property Rights law, including copyright law. Copyright and IPR is retained by the creators or other copyright holders. Terms and conditions for use of this material are defined in the End User Agreement.

University of Reading

www.reading.ac.uk/centaur

CentAUR

Central Archive at the University of Reading

Reading's research outputs online

Intensified Impact of Tropical Atlantic SST on the Western North Pacific Summer Climate Under a Weakened Atlantic Thermohaline Circulation

Wei Chen[1], June-Yi Lee[2], Riyu Lu[1], Buwen Dong[3] and Kyung-Ja Ha[2,4]

[1.] State Key Laboratory of Numerical Modeling for Atmospheric Sciences and Geophysical Fluid Dynamics, Institute of Atmospheric Physic, Chinese Academy of Sciences, Beijing, China

[2.] Institute of Environmental Studies, Pusan National University, Busan, Korea

[3.] National Centre for Atmospheric Science-Climate, Department of Meteorology, University of Reading, Reading, UK

[4.] Department of Atmospheric Sciences, Pusan National University, Busan, Korea

Submitted to Climate Dynamics

Corresponding author:
Dr. Kyung-Ja Ha
Department of Atmospheric Sciences
Pusan National University
Busan, 609-735, Korea
Email: kjha@pusan.ac.kr

Abstract

The tropical North Atlantic (TNA) sea surface temperature (SST) has been identified as one of regulators on the boreal summer climate over the western North Pacific (WNP), in addition to SSTs in the tropical Pacific and Indian Oceans. The major physical process previously proposed is that the TNA warming induces a pair of cyclonic circulation anomaly over the eastern Pacific and negative precipitation anomalies over the eastern to central tropical Pacific, which in turn lead to an anticyclonic circulation anomaly over the western to central north Pacific. This study further demonstrates that the modulation of the TNA warming to the WNP summer climate anomaly tends to be intensified under background of the weakened Atlantic thermohaline circulation (THC) by using a water-hosing experiment. The result suggests that the weakened THC induces a decrease in thermocline depth over the TNA region that results in enhanced sensitivity of SST variability to wind anomalies and thus intensification of the interannual variation of TNA SST. Under the weakened THC, the atmospheric responses to the TNA warming are westward shifted, enhancing the anticyclonic circulation and negative precipitation anomaly over the WNP. This result supports the recent finding that the negative phase of the Atlantic multidecadal oscillation (AMO) after the late 1960s has been favourable for the strengthening of the connection between TNA SST variability and WNP summer climate and has important implications for seasonal prediction and future projection

of the WNP summer climate.

Key words: western North Pacific (WNP) summer climate; tropical North Atlantic (TNA) SST; weakened Atlantic thermohaline circulation (THC); Atlantic multidecadal oscillation (AMO)

1. Introduction

The western North Pacific (WNP) summer climate, as one of the most important components in the Asian summer monsoon system, has been widely studied. The WNP anticyclonic circulation (WNPAC) is closely related with the East Asian monsoon in subseasonal to seasonal time scales (Kosaka et al. 2013; Lee et al. 2013; Moon et al. 2013; Wang et al. 2014) and tropical storm (Wang et al. 2013). Thus, better understanding of the WNPAC variability is of particular importance in understanding the Asian summer monsoon system that is the most difficult challenge in seasonal climate prediction (e.g., Kang et al. 2004; Wang et al. 2004, 2009, 2014; Lee et al. 2010, 2011b; Kosaka et al. 2012; Sohn et al. 2012 and many others).

The WNPAC variability is mainly influenced by the El Niño Southern Oscillation (ENSO; e.g., Chang et al. 2000; Wang et al. 2000, 2013; Chou et al. 2003; Wu et al. 2003; Yun et al. 2013; Lee et al. 2011a,b, 2014). Wang et al. (2000, 2013) pointed out that El Niño heating over the central and eastern equatorial Pacific leads to an anomalous WNPAC. In addition, the sea surface temperature (SST) anomaly in the Indian Ocean, following the El Niño events, contributes to the persistence of WNPAC

(e.g., Yang et al. 2007; Li et al. 2008; Xie et al. 2009; Ding et al. 2010; Yun et al. 2010; Chowdary et al. 2010, 2014; Kosaka et al. 2013). Thus, previous studies have focused mainly on the impacts of ENSO-related SST anomalies over the Pacific Ocean and Indian Ocean and less attention has been paid on the Atlantic Ocean.

There is increasing evidence of the remote impact of Atlantic Ocean on the tropical Pacific Ocean and ENSO events (e.g., Rodriguez-Fonseca et al. 2009; Ding et al. 2012; Kucharski et al. 2011; Ham et al. 2013; Hong et al. 2013). Kucharski et al. (2011) showed that the warming over the Atlantic Ocean modulates the mean atmospheric field over the tropical Pacific by inducing an anomalous Walker circulation and leads to a cooling over the eastern tropical Pacific. Ham et al. (2013) suggested that the SST anomaly over the tropical north Atlantic (TNA) could be a trigger for El Niño events by inducing an atmospheric teleconnetion over the tropical Pacific.

Moreover, for the modulation of TNA SST on the WNP summer climate, Hong et al. (2013) pointed out that the TNA warming could induce strong easterly and increased precipitation anomalies over the eastern to central Pacific by using an atmospheric general circulation model (AGCM). They highlighted the role of local moisture feedback over the warm pool region in response to the TNA forcing rather than the detailed mechanism of the teleconnection between TNA SST and WNP summer climate. In addition, Hong et al. (2014) argued an enhancement of relationship between TNA SST and WNP summer climate after the early 1980s.

However, the detailed mechanisms responsible for this decadal change have not been fully elucidated.

The connection between the Atlantic Ocean and Pacific Ocean has been increased since the late 1960s (Polo et al. 2008; Rodriguez-Fonseca et al. 2009). This increased relationship in the late 1960s seems to concur with a negative phase of the Atlantic multidecadal oscillation (AMO) in observations (Knight et al. 2005), suggesting that AMO might be an important factor that modulates the relationship between Atlantic and Pacific. In addition, as a leading mode of multidecadal SST variability, the AMO has influence not only on the Atlantic region but also on other ocean basins (e.g., Dong et al. 2006; Sutton and Hodson 2007; Li et al. 2008).

The observational records reveal a negative AMO phase during the late 1960s to the 1990s, followed by a positive phase after the late 1990s (Knight et al. 2005). The fluctuation of AMO can arise through the variation of Atlantic thermohaline circulation (THC; e.g., Delworth and Mann 2000; Curry et al. 2003; Zhai and Sheldon 2012), although there is also evidence that changes in natural (e.g. volcanic) or anthropogenic (aerosols) external forcing can exert an important influence (e.g., Ottera et al. 2010; Booth et al. 2012; Zhang et al. 2013). Furthermore, by using coupled models, a substantially weakened THC could produce a negative phase of AMO through a water-hosing experiment in which an extra freshwater flux is artificially applied in the North Atlantic (e.g., Dong and Sutton 2002; Dahl et al. 2005; Zhang and Delworth 2005; Dong and Sutton 2007, Haarsma et al. 2008; Laurian et al.

2009; Lu and Dong 2008; Lu et al. 2008).

The weakened THC significantly influences both the mean states and interannual variability of SST over the Atlantic (e.g., Polo et al. 2013). The climatological SST changes exhibit as a cooling in the North Atlantic and a warming in the South Atlantic, because of the pronounced decrease of northward ocean heat transport under the weakened THC (e.g., Dong and Sutton 2002; Dahl et al. 2005; Zhang and Delworth 2005; Timmermann et al. 2007). In addition, the interannual variability of SST over the Atlantic Ocean can be modulated by the weakened THC (Haarsma et al. 2008; Polo et al. 2013). Polo et al. (2013) suggested an enhancement of tropical Atlantic variability in boreal late spring-early summer, which is due to an increase in the variance of wintertime ENSO through affecting anomalous surface heat fluxes.

Furthermore, the changes in the Atlantic Ocean under the weakened THC could be extended to the Pacific. The SST anomalies over the Atlantic modulate the mean states of wind filed over the tropical Pacific by the atmospheric bridge (e.g., Zhang and Delworth 2005; Timmermann et al. 2007). In addition, this modulation further affects the ENSO variability (Dong and Sutton 2007), the mean states of Asian summer monsoon (Lu and Dong 2008) and the relationship between ENSO and south Asian summer monsoon (Lu et al. 2008).

This study demonstrates how the impacts of TNA SST on the WNP summer climate are strengthened under the background of weakened THC by comparing a water-hosing sensitivity experiment with a control simulation. The model and

104 experiments are described in Section 2. The robust impacts of TNA SST on the WNP
105 summer climate are first assessed in observations in Section 3. Section 4 demonstrates
106 the changes of TNA SST variability affecting WNP summer climate by the weakened
107 THC and Section 5 provides the observed evidence. The summary and discussion are
108 given in Section 6.

109 **2. Model and experiment**

110 The third version of the Hadley Centre Coupled Ocean–Atmosphere General
111 Circulation Model (HadCM3; Gordon et al. 2000) is used in this work. The
112 atmospheric component of HadCM3 has 19 levels with a horizontal resolution of 2.5°
113 latitude by 3.75° longitude (Pope et al. 2000), and the oceanic component has 20
114 levels with a horizontal resolution of 1.25° by 1.25°. The control simulation (CNTL)
115 uses pre-industrial atmospheric trace gas concentrations and incoming solar radiation
116 providing the only external forcing and maintains a stable climate (Gordon et al.
117 2000).

118 A water-hosing experiment (1Sv hereafter) is performed in which an extra
119 freshwater flux of 1.0 Sv (1 Sv=10^6 m^3 s^{-1}) is applied uniformly for 100 years to the
120 ocean surface of the North Atlantic between 50°N and 70°N. The external fresh water
121 flux is then switched off after model year 100 and integration continues for an
122 additional 100 years. This experiment is started with the same initial condition with
123 the CNTL (see more details from Dong and Sutton (2007)). The 1.0 Sv freshwater

124 flux leads to quickly decrease of THC in the first four decades. After that, a stable
125 strength of THC, with a 70% weakening in comparison with that in the CNTL, is kept
126 for the last integration years (Dong and Sutton 2007). In this study, we analyze the
127 last 160 years of the 1Sv and compare with a parallel CNTL to highlight the impacts
128 of TNA SST anomaly on the WNP summer climate under the weakened THC. The
129 same simulations have been used to investigate the impacts of the weakened THC on
130 the interannual variability of TNA SST (Polo et al. 2013), the ENSO variability (Dong
131 and Sutton 2007), and the Asian summer monsoon climate (Lu and Dong 2008).

132 In addition, the observational datasets used in this study include the Hadley
133 Centre sea ice and sea surface temperature (HadISST; Rayner et al. 2003) with a
134 horizontal resolution of 1° by 1°) for the period of 1948–2012, and lower-tropospheric
135 circulation data from the National Centers for Environmental Prediction
136 (NCEP)/National Center for Atmospheric Research (NCAR) reanalysis data with
137 horizontal resolution of 2.5° by 2.5° (Kalnay et al. 1996) within the same period.
138 Boreal summer June, July and August (JJA) is a major target season in this study.

139 **3. Robust influence of Atlantic SST on the WNP**

140 Figure 1 exhibits spatial distribution of JJA-mean SST anomalies related to the
141 WNPAC with and without ENSO influence, respectively, during the period of
142 1967–1997 when the AMO was in a negative phase in observations. Here, the strength
143 of WNPAC is defined by averaging 850-hPa stream-function anomalies over the

144 region of 0°−25°N, 110°−145°E following Li et al. (2007). The strong WNPAC tends
145 to be associated with (1) the negative SST anomaly over the central and eastern
146 tropical Pacific, (2) the positive SST anomaly over the WNP and the North Indian
147 Ocean (NIO), and (3) the positive SST anomaly over the TNA as shown in Fig. 1a.
148 The relative contributions of simultaneous SST anomaly over different ocean regions
149 can be demonstrated by their correlation coefficients with the WNPAC index (Table.
150 1). The WNPAC is mainly correlated with the SST anomaly over the central (Niño 4:
151 SST anomalies averaged over 5°S−5°N, 160°E−150°W) and the eastern (Niño 3: SST
152 anomalies averaged over 5°S−5°N, 90°−150°W) tropical Pacific, which can be
153 recognized as strong ENSO signals. The SST over the TNA (averaged over 0°−20°N,
154 30°−80°W) plays a secondary role in the WNPAC, which is relatively weak,
155 compared with those associated with the ENSO signals. In addition, the SST anomaly
156 over the NIO (5°−20°N, 40°−100°E) and the WNP (5°−25°N, 110°−160°E) also
157 contribute to the WNPAC.

158 It is noted that the contribution of TNA SST to the WNPAC is intensified after
159 removing the ENSO influence. We use the Niño 4 index to represent the ENSO signal,
160 since it not only has the strongest influence on the WNPAC, but also has the closest
161 relationship with both SST anomalies over the eastern tropical Pacific and Indian
162 Ocean (Table. 1). The impacts of Niño 4 SST are first eliminated by using the linear
163 regression for the original SST and circulation field with respect to the Niño 4 index,
164 and then the WNPAC and SST indices, as well as the regression analysis, are

165 recalculated. The relationship between the TNA SST and WNPAC index is greatly
166 enhanced after the impacts of Nino 4 SST are removed, with a significant correlation
167 coefficient of 0.506 in comparison with 0.344 before. On the contrary, the correlation
168 coefficient of the WNPAC with the Niño 3 index sharply decreased. In addition, the
169 correlation coefficient of WNPAC index with the TNA SST index is also stronger than
170 its correlations with NIO and WNP SST indices, although they have somewhat
171 increased, compared with originals. The results indicate that the WNP summer
172 climate could depends on the SST anomaly over the TNA in addition to the tropical
173 Pacific and Indian Oceans.

174 Figure 1b shows the regressions of SST anomalies onto the WNPAC index after
175 excluding the impacts of the Niño 4 index. In comparison with the original SST
176 anomalies shown in Fig. 1a, SST anomalies over the tropical Pacific are considerably
177 weakened since the SST pattern related to ENSO has been removed. Moreover, the
178 SST over the TNA is enhanced, with a normalized SST anomaly increasing from 0.23
179 to 0.33. This figure indicates that the WNPAC is mainly related to the SST anomaly
180 over the TNA after excluding the impacts of Niño 4 SST. Thus, in the following part,
181 in order to show the robust impact of TNA SST anomaly on the WNP summer climate,
182 the ENSO effect is first removed by using the linear regression with respect to the
183 Niño 4 index.

184 To clearly demonstrate the variation of TNA SST and WNPAC indices and their
185 relationship, Fig. 2 shows the time series of these two indices during the period of

1967–1997. The figure indicates large interannual variability for the TNA SST and WNPAC indices. The positive correlation means that a TNA warming (cooling) is associated with anomalous anticyclonic (cyclonic) circulation over the WNP. Furthermore, after removing the impacts of Niño 4 SST, this positive correlation is significantly enhanced, indicating an intensified relationship between TNA SST variability and the WNPAC without ENSO.

To illustrate causality , Fig. 3 shows the lead-lag correlation between monthly-mean TNA SST and JJA-mean WNPAC indices, following Svendsen et al. (2013). A significant positive correlation coefficient starts when TNA SST index is leading seven month (Previous December). And the correlation coefficients are stronger when the TNA SST is leading than those when the WNPAC is leading. The results suggest that the TNA SST variability might be a cause for the WNPAC. Moreover, the correlation between TNA SST and WNPAC are significant intensified from spring to summer after eliminating the Niño 4 SST impacts, which further indicates that the modulation of TNA SST on the WNPAC is enhanced without ENSO influence.

Figure 4 shows the SST anomalies associated with the WNPAC in the CNTL. The model can reproduce the WNPAC-associated positive SST anomaly over the TNA and Indian Ocean and the negative SST anomaly over the central and eastern tropical Pacific, although the ENSO signal is extended to the western Pacific likely due to the error of cold tongue extending too far westward in the coupled model

(Collins et al. 2001). After excluding the impacts of Niño 4 SST (Fig. 4b), on the one hand, the area with significant positive SST anomaly over the TNA is broadened with an intensified strength (the normalized TNA SST anomaly increases from 0.05 to 0.12). On the other hand, the SST anomalies over the tropical Pacific are weakened [normalized Niño 4 (Niño 3) varies from -0.33 (-0.20) to 0.01 (0.09)]. Thus, the CNTL not only captures the TNA warming associated with strong WNPAC, but also reproduces the enhanced warming after excluding the impacts of Niño 4 signal, although the model slightly underestimates the strength of positive SST anomaly over the TNA.

4. The impacts of the weakened THC

4.1 Mean and variability of the TNA SST

The impacts of the weakened THC on the TNA SST are first investigated by comparing the 1Sv and CNTL results for 160 years. The difference of climatological mean SST between the 1Sv and CNTL indicates that the SST response in the Atlantic Ocean to the weakened THC is characterized by an interhemispheric asymmetry with a cooling over the northern hemisphere and a warming over the southern hemisphere (Fig. 5a). The North Atlantic SSTs decrease in a range from 1.0° to 5.0°C over the region south of 45°N. The southern Atlantic warms by about 1.0°C–1.5°C, because of decreased northward ocean heat transport under the weakened THC (Stouffer et al. 2006). This cooling of the North Atlantic and warming of the South Atlantic is

consistent with previous coupled modeling studies (Dong and Sutton 2002; Dahl et al. 2005; Zhang and Delworth 2005) and with the multi-model results of Timmermann et al. (2007). In addition to the local SST response, the weakened THC also induces a cooling (about 1.0 °C) in the eastern tropical Pacific, which is associated with a shallow thermocline there (Dong and Sutton 2007).

Figures 5b shows the differences of SST standard deviation between the two experiments for the original SST field. Under the weakened THC, the interannual variability of North Atlantic shows a significant enhancement. The increase of amplitude for the TNA region is 0.55°C (from 0.33°C in the CNTL to 0.88 in the 1Sv). In addition, the standard deviation of SST over the tropical eastern Pacific also increases, which indicates the intensification of ENSO variability in the 1Sv (Dong and Sutton 2007). Furthermore, after removing the ENSO impact by using the Niño 4 index, the interannual variability of North Atlantic still increases in the 1Sv (Fig. 5c), although the TNA SST is influenced partly by the ENSO variability (Alexander and Scott 2002; Chiang and Sobel 2002). Over the TNA region, the standard deviation is increased by 159% from 0.32°C to 0.83°C. The enhancement of TNA SST variability without ENSO impacts might be due to the shallow thermocline and increased thermocline feedback over the TNA under the weakened THC, because of the decrease in the thermocline depth over the TNA (not shown). This is consistent with Tokinaga and Xie (2011), who suggested that the local thermocline feedback is another factor to affect the internnual variability over the tropical Atlantic besides

ENSO. The enhancement for interannual variability of the TNA SST under the weakened THC has been argued in Polo et al. (2013). In their study, however, the increase in interannual tropical Atlantic variability is contributed by the intensified ENSO variability. Our study further demonstrates the TNA variability independent from ENSO can also be enhanced under the background of the weakened THC. In short, both the mean states and interannual variability of SST over the TNA are significantly changed under the weakened THC.

4.2 Impact on the WNP summer climate

This section discusses changes in the response of the WNPAC and WNP climate to the TNA SST variability under the weakened THC by comparing the 1Sv and CNTL. ENSO-related variability is removed in all of the analyses. Figure 6 shows the regression patterns of lower-tropospheric stream-function onto the TNA index in the two experiments. In the CNTL, the TNA warming is associated with a pair of cyclonic anomalies located from the eastern Pacific to the western Atlantic and a pair of anticyclonic anomalies that occurred in the western to central Pacific (Fig. 6a). This wave-like pattern indicates a remote connection between the TNA and WNP. Figure 6b indicates that the circulation anomalies associated with the TNA warming exhibit a westward shift in the 1Sv. The central area for the cyclonic anomalies moves to the eastern Pacific and that for the anticyclonic anomalies moves to the western Pacific. Particularly, the WNPAC is significantly intensified in the 1Sv. The strength

of the WNPAC is 0.81×10^6 $m^2 s^{-1}$ in the CNTL, but is 1.33×10^6 $m^2 s^{-1}$ in the 1Sv. The enhancement of WNPAC indicates that the impacts of TNA SST on the WNP summer climate are intensified by the weakened THC.

Figure 7 shows the pattern of 200-hPa velocity potential related to the TNA index in the two experiments. The results further indicate a westward shift in the atmospheric response to the TNA warming under the weakened THC. Corresponding with the lower-tropospheric circulation anomaly, the upper troposphere also exhibits a wave-like pattern with a divergence over the eastern Pacific to Atlantic Ocean and a convergence over the western to central Pacific both in the CNTL and 1Sv, indicating the role of large scale tropical divergent circulation for the connection between the TNA SST and the WNP summer climate (e.g., Kucharski et al. 2011, Hong et al. 2013). However, this pattern extends westward in the 1Sv. The central area of convergence shifts westward from the eastern tropical Pacific to the central tropical Pacific, and therefore the strength of convergence over the WNP is intensified. The results suggest that the tropical Atlantic and Pacific could be connected by a Walker circulation anomaly induced by the TNA warming. Moreover, this Walker circulation anomaly is westward extended and results in an intensified relationship between TNA SST and WNP summer climate in the 1Sv, in compared to the CNTL.

Figure 8 shows the precipitation and 850-hPa wind anomalies associated with the TNA index. In the CNTL, the TNA warming enhances the local convection activity and leads to a strong positive precipitation anomaly over the TNA and eastern tropical

289 Pacific. The western boundary of the positive precipitation anomaly is limited east of
290 110°W (Fig. 8a). The associated diabatic heating gives rise to a pair of
291 lower-tropospheric cyclonic anomalies over its western side (Fig. 6a) as a Gill-pattern
292 Rossby wave response, which generates northeasterly on the western flank (Fig. 8a).
293 This wind anomaly is associated with a negative precipitation anomaly over the
294 central and eastern tropical Pacific through enhancing the wind speed, dry advection
295 (Xie 1999; Ham 2007) and resultant anomalous sinking motion (Fig. 7a). Furthermore,
296 the negative precipitation anomaly induces a pair of anticyclonic anomalies over the
297 western to central Pacific (Fig. 6a), with northerly flow on its eastern edge (Fig. 8a),
298 which further reinforces the negative precipitation anomaly. This strong positive
299 feedback between the precipitation and wind anomaly delivers the influence of the
300 Atlantic on the Pacific. It should be mentioned that Ham et al. (2013) has suggested
301 similar physical processes taking place in spring. Our study further indicates that the
302 connection between TNA SST and WNP climate by the atmospheric teleconnetion
303 also occurs in summer.

304 Figure 8b shows that the changes in precipitation and lower-tropospheric wind
305 anomaly associated with the TNA warming also occur in the 1Sv. The positive
306 precipitation anomalies in response to the TNA warming extend to the eastern
307 equatorial Pacific, with the west edge around 120°W (Fig. 8b). The corresponding
308 cyclonic anomaly extends to the eastern Pacific (Fig. 6b), which leads to the
309 anomalous sinking motion moving to the central tropical Pacific (Fig. 7b) and the

310 negative precipitation anomaly shifting westward to the central to western tropical
311 Pacific (Fig. 8b). As a result, the anticylonic anomaly over the WNP, as well as the
312 local negative precipitation anomaly, is intensified (Fig. 8b).

313 The TNA SST anomaly and the WNP summer climate are linked by a coupled
314 interaction between convection and circulation. It can be explained as follows: the
315 TNA warming induces a pair of cyclonic circulation anomaly over the eastern Pacific
316 and negative precipitation anomaly over the eastern to central tropical Pacific, which
317 in turn leads to an anticyclonic circulation anomaly over the western to central north
318 Pacific. These processes occur both in CNTL and 1Sv, acting as a bridge to relay the
319 impacts of Atlantic to the WNP. However, in the 1Sv, the coupled interaction is
320 shifted westward and tends to enhance the WNPAC.

321 Figure 9 shows the SST anomalies related to the TNA warming, which could
322 explain the westward shift of teleconnection pattern associated with the TNA SST
323 change. Because the ENSO signal has been eliminated first, the strong SST anomaly
324 is mainly confined over the North Atlantic in the CNTL (Fig. 9a). In addition, the
325 cooling over the subtropical eastern Pacific is associated with the strong negative
326 precipitation there (Fig. 8a). In the 1Sv, however, associated with the TNA warming is
327 positive SST anomalies over the eastern tropical Pacific (Fig. 9b). These positive SST
328 anomalies are the response to the westward shift of coupled interaction over the
329 Pacific. The warming in the eastern tropical Pacific is caused by the westerly flow
330 over the equatorial eastern Pacific (Fig. 8b) through decreasing the easterly trades and

suppressing the local upwelling. Even though this westerly flow also exists in the CNTL, the thermocline over the equatorial eastern Pacific is shallower under the weakened THC as illustrated in (Fig. 10. It can been seen that the thermocline depth over the eastern equatorial Pacific is significantly decreased in the 1Sv with the difference of D20 over the region 5°S−5°N, 60°−95°E of -16.37 m. The change of thermocline depth over the tropical Pacific under the weakened THC is contributed to by the anomalous Ekman pumping, associated with the anomalous wind stress (Dong and Sutton 2007). Over the eastern tropical Pacific, the shallow thermocline in the 1Sv is due to the increased Ekman upwelling induced by the local easterly wind stress. The shallower thermocline over the equatorial eastern Pacific increases the sensitivity of SST variability to local wind change. Therefore, the change of thermocline depth over the eastern Pacific under the weakened THC plays a crucial role in the enhancement of the impacts of TNA SST on the WNP summer climate by westward shift of coupled interactions among SST, convection and circulation over the tropical Pacific.

5. Observational evidence

Our finding of intensification in the impacts of the TNA SST on the WNPAC under the weakened THC is further confirmed by observational evidence. Here a positive AMO is combined by two periods of 1948–1966 and 1998–2012 (total of 34 years), comparing with a negative AMO represented by the period of 1967–1997 (31

351 years). The linkage between the TNA SST and WNPAC in the positive phase of AMO
352 is weaker than that in the negative phase of AMO in observations. The correlation
353 coefficient between the TNA SST and WNPAC without ENSO influence is only 0.265
354 during the positive AMO, in contrast to a significant one of 0.506 in the negative
355 AMO. The results indicate that the negative phase of AMO, most likely related to a
356 weakened THC, is more in favour for a strong teleconnection between the TNA SST
357 and WNP summer climate than the positive AMO.

358 Figure 11 shows the circulation response to the TNA warming during the
359 negative and positive AMO phases, respectively. The enhancement in the connection
360 between the TNA SST and the WNPAC is further indicated by the strong circulation
361 anomalies over the WNP during the negative AMO than those during the positive one.
362 In the lower troposphere, the TNA warming induces a cyclonic anomaly over the
363 eastern tropical Pacific and an anticyclonic anomaly over the WNP in both negative
364 and positive AMO (Figs. 11a and c). However, the WNPAC shown in Fig. 11a is
365 strong and well organized, indicating a strong response of the WNP summer climate
366 to the TNA SST during the negative AMO, similar to those in the 1Sv (Fig. 6b). In the
367 period of the positive AMO, however, the circulation anomaly associated with the
368 TNA warming is much weaker (Fig. 11b). The weakened WNPAC implies a decrease
369 in the teleconnection between TNA and WNP during the positive AMO. The stronger
370 circulation response to the TNA warming in the negative AMO than that in the
371 positive AMO also shows in the upper troposphere. The convergence over the tropical

Pacific is strong and extends to the WNP in the negative AMO (Fig. 11c), in comparison with a weakened one in the positive AMO (Fig. 11d). Thus, the strong linkage between the TNA SST and WNP summer climate in the negative AMO during the late 1960s–1990s further confirms that the weakened THC (a negative AMO) provides a favorable background for the enhancement of the teleconnection between TNA SST and the WNPAC.

6. Summary and discussion

By using two experiments (CNTL and 1Sv) with the HadCM3, this study demonstrates that the impacts of the TNA warming on the WNP summer climate tend to be intensified under the background of the weakened THC (the negative AMO phase in other word). Observational analysis also confirms modeling results.

The WNP summer climate is mainly regulated by the SST anomaly over the tropical Pacific, the Indian Ocean and the TNA in observations. However, the SST variabilities over the Indian Ocean and tropical Pacific are closely correlated with each other, as well as with TNA SST variability. After excluding the ENSO influence, the relationship between the TNA SST and WNPAC is greatly intensified, highlighting the influence of the TNA SST on the WNP summer climate.The TNA warming is associated with anomalous WNPAC during summer. The physical processes connecting the TNA and the WNP are illustrated by the CNTL. On the one hand, the TNA warming is associated with anomalous divergence from the eastern

392 Pacific to Atlantic Ocean and anomalous convergence from the western to central
393 Pacific in the upper troposphere, indicating the role of large scale tropical divergent
394 circulation for the connection between the TNA SST and the WNP summer climate.
395 On the other hand, the positive SST anomaly over the TNA enhances the local
396 convection which gives rise to a cyclonic anomaly over the eastern Pacific by
397 inducing anomalous diabatic heating. The northeasterly flow on the western edge of
398 the cyclonic anomaly contributes to a negative precipitation over the eastern to central
399 tropical Pacific, which in turn generates the anticyclonic anomaly over the western to
400 central tropical Pacific. Moreover, the circulation and precipitation anomalies over
401 the tropical Pacific have a positive feedback to intensify each other. Therefore, the
402 coupled convection–circulation interaction over the Pacific associated with the TNA
403 SST anomaly delivers the impacts of TNA SST to the WNP.

404 The impacts of TNA SST on the WNP summer climate are intensified under the
405 weakened THC. In the 1Sv, the WNPAC and associated precipitation anomaly
406 response to the TNA warming are enhanced. This enhancement is due to the westward
407 shift of the teleconnection pattern related to the TNA SST. Under the weakened THC,
408 the thermocline over the eastern equatorial Pacific is shallower than that in the CNTL.
409 The shallow thermocline increases the sensitivity of SST to surface wind anomalies in
410 the eastern tropical Pacific. Meanwhile, the circulation and precipitation anomalies
411 associated with TNA warming are shifted westward. Especially, the anticyclonic
412 anomaly moves to the western Pacific, which leads to an enhanced WNPAC and

strong negative precipitation anomaly there. This result indicates the role of changes in mean states over the equatorial eastern Pacific by the weakened THC in increasing the influence of TNA SST on the WNP summer climate.

It should be noted that the physical processes is obtained through the positive TNA SST anomaly by linear regression analysis, but it also makes physical sense for the negative TNA SST anomaly. The composite analysis of negative TNA SST anomaly (not shown) suggested that the TNA cooling leads to a cyclonic circulation anomaly over the western to central north Pacific in the CNTL. Moreover, under the weakened THC, the TNA cooling extends to the eastern tropical Pacific, and the atmospheric response to the TNA cooling are westward shifted and therefore enhances the cyclonic circulation and positive precipitation anomaly over the WNP. Thus, TNA cooling also have stronger impacts in the 1Sv than those in the CNTL.

In addition, considering theNiño 3 SST variability is strongest in DJF over the tropical Pacific, the circulation response to the TNA after removing the impacts of DJF-mean Niño 3 variability is also investigated. The results indicate the WNPAC is intensified in the 1Sv without the impacts of SST over the eastern tropical Pacific. These indicate that the main conclusions are robust and they are not sensitive to how the ENSO impacts are removed.The intensification in the impacts of TNA SST on the WNPAC under the weakened THC is further confirmed by the stronger connection between the TNA SST and the WNPAC in a negative phase of AMO than that in a positive one in observations. During the late 1960s–1990s characterized as a negative

AMO, the TNA SST is closely related to the WNP by inducing a strong WNPAC. However, it should be mentioned that in observations, the circulation anomalies associated with TNA warming do not exhibit a clear westward shift during the negative phase of AMO, unlike the simulations, possibly due to the smaller sampling size in observations and weaker SST anomalies associated with AMO compared with those associated with substantial weakened THC.

The results presented in this study indicate the importance of the Atlantic SST anomaly in modulating the WNP summer climate via a tropical teleconnection. Furthermore, the changes in mean states on decadal timescale can modulate this impact. Thus, more attention should be paid on the Atlantic SST for improving the seasonal prediction of WNP summer climate.

Acknowledgements

This study was supported by the National Natural Science Foundation of China (Grant Nos. 41105046 and 41320104007).

Reference

Alexander MA, Scott JD (2002) The influence of ENSO on air-sea interaction in the Atlantic. Geophys Res Lett 29:1701. doi:10.1029/2001GL014347

Booth BB, Dunstone NJ, Halloran PR, Andrews T, Bellouin N (2012) Aerosols implicated as a prime driver of twentieth-century North Atlantic climate variability. Nature 484:228–233

Chang CP, Zhang YS, Li T (2000) Interannual and interdecadal variations of the East Asian summer monsoon and tropical Pacific SSTs. Part I: Roles of the subtropical ridge. J Clim 13:4310–4325

Chiang JCH, Sobel AH (2002) Tropical tropospheric temperature variations caused by ENSO and their influence on the remote tropical climate. J Clim 15:2616–2631

Chou C, Tu JY, Yu JY (2003) Interannual variability of the western North Pacific summer monsoon: differences between ENSO and non-ENSO years. J Clim 16:2275–2287

Chowdary JS, Xie SP, Lee JY, Kosaka Y, Wang B (2010) Predictability of summer Northwest Pacific climate in 11 coupled model hindcasts: local and remote forcing. J Geophys Res 115: D22121

Chowdary JS, Attada R, Lee JY, Kosaka Y et al (2014) Seasonal prediction of distinct climate anomalies in the summer 2010 over the tropical Indian Ocean and South Asia. J Meteorol Soc Jpn 92: 1-16

Collins M, Tett SFB, Cooper C (2001) The internal climate variability of HadCM3, a version of the Hadley Centre coupled model without flux adjustments. Clim Dyn 17:61–81

Curry R, Dickson B, Yashayaev I (2003) A change in the freshwater balance over the Atlantic Ocean over the past four decades. Nature 426:826–829

Dahl KA, Broccoli AJ, Stouffer RJ (2005) Assessing the role of North Atlantic freshwater forcing in millennial scale climate variability: a tropical Atlantic perspective. Clim Dyn 24:325–346. doi:10.1007/s00382-004-0499-5

Delworth TL, Mann ME (2000) Observed and simulated multidecadal variability in the Northern Hemisphere. Clim Dyn 16:661–676. doi:10.1007/s003820000075

Ding H, Keenlyside NS, Latif M (2012) Impact of the equatorial Atlantic on the El Niño Southern oscillation. Clim Dyn 38:1965–1972. doi:10.1007/s00382-011-1097-y

Ding R, Ha KJ, Li J (2010) Interdecadal shift in the relationship between the East Asian summer monsoon and the tropical Indian Ocean. Clim Dyn 34:1059–1071. doi:10.1007/s00382-009-0555-2

Dong B, Sutton RT (2002) Adjustment of the coupled oceanatmosphere system to a sudden change in the thermocline circulation. Geophys Res Lett 29:1728. doi:10.1029/2002GL015229

Dong B, Sutton RT (2007) Enhancement of ENSO variability by a weakened Atlantic thermocline circulation in a coupled GCM. J Clim 20:4920–4939

491 Dong B, Sutton RT, Scaife AA (2006) Multidecadal modulation of El Niño-Southern
492 Oscillation (ENSO) variance by Atlantic Ocean sea surface temperatures.
493 Geophys Res Lett 33:L08705. doi:10.1029/2006GL025766
494 Gordon C, Cooper C, Senior CA, Banks H, Gregory JM, Johns TC, Mitchell JFB,
495 Wood RA (2000) The simulation of SST, sea ice extents and ocean heat transports
496 in a version of the Hadley Centre coupled model without flux adjustments. Clim
497 Dyn 16:147–168.
498 Haarsma RJ, Campos E, Hazeleger W, Severijns C (2008) Influence of the meridional
499 overturning circulation on tropical Atlantic climate and variability. J Clim
500 21:1403–1416
501 Ham YG, Kug JS, Kang IS (2007) Role of moist energy advection in formulating
502 anomalous Walker Circulation associated with ENSO. J Geophy Res 112:D24105.
503 doi:10.1029/2007JD008744
504 Ham YG, Kug JS, Park JY, Jin FF (2013) Sea surface temperature in the north tropical
505 Atlantic as a trigger for El Niño/Southern Oscillation events. Nat Geosci
506 6(2):112–116. doi:10.1038/ngeo1686
507 Hong CC, Chang TC, Hsu HH (2014) Enhanced relationship between the tropical
508 Atlantic SST and the summertime western North Pacific subtropical high after
509 the early 1980s. J Geophys Res doi:10.1002/2013JD021394
510 Hong S, Kang IS, Choi I, Ham YG (2013) Climate responses in the tropical Pacific
511 associated with Atlantic warming in recent decades. Asia-Pac J Atmos Sci

512 49:209–217
513 Kalnay E, Kanamitsu M, Kistler R et al (1996) The NCEP/NCAR 40-Year Reanalysis
514 Project. Bull. Amer Meteor Soc, 77:437–471
515 Knight JR, Allan RJ, Folland CK, Vellinga M, Mann ME (2005) A signature of
516 persistent natural thermohaline circulation cycles in observed climate. Geophys
517 Res Lett 32:L20708. doi:10.1029/2005GL024233
518 Kang IS, Lee JY, Park CK (2004) Potential predictability of summer mean
519 precipitation in a dynamical seasonal prediction system with systematic error
520 correction. J Clim 17: 834–844
521 Kosaka Y, Chowdary JS, Xie SP, Min YM, Lee JY (2012) Limitations of seasonal
522 predictability for summer climate over East Asia and the Northwestern Pacific. J
523 Clim 25: 7574-7589
524 KosakaY, Xie SP, Lau NC, Vecchi GA (2013) Origin of seasonal predictability for
525 summer climate over the Northwestern Pacific. PNAS 110: 7574-7579
526 Kucharski F, Kang IS, Farneti R, Feudale L (2011) Tropical Pacific response to 20th
527 century Atlantic Warming. Geophys Res Lett 38:L03702,
528 doi:10.1029/2010GL046248
529 Laurian A, Drijfhout SS, Hazeleger W, van Dorland R (2009) Global surface cooling:
530 the atmospheric fast feedback response to a collapse of the thermohaline
531 circulation. Geophys Res Lett 36:L20708. doi:10.1029/2009GL040938
532 Lee JY, Wang B, Seo KH, Kug JS, Choi YS, Kosaka Y, Ha KJ (2014) Future change

533 of Northern Hemisphere summer tropical-extratropical teleconnection in CMIP5
534 models. J Clim in press. Doi:10.1175/JCLI-D-13-00261.1
535 Lee JY, Wang B, Wheeler MC, Fu X, Waliser DE, Kang IS (2013) Real-time
536 multivariate indices for the boreal summer intraseasonal oscillation over the
537 Asian summer monsoon region. Clim Dyn, 40: 493–509
538 Lee JY, Wang B, Ding Q, Ha KJ, Ahn JB, Kumar A, Stern B, Alves O (2011a) How
539 predictable is the Northern Hemisphere summer upper-tropospheric circulation?
540 Clim Dyn 37: 1189–1203.
541 Lee JY, Wang B, Kang IS, Shukla J et al (2010) How are seasonal prediction skills
542 related to models' performance on mean state and annual cycle? Clim Dyn
543 35:267–283
544 Lee SS, Lee JY, Ha KJ, Wang B, Schemm JKE (2011b) Deficiencies and possibilities
545 for long-lead coupled climate prediction of the western North Pacific-East Asian
546 summer monsoon. Clim Dyn 36: 1173–1188
547 Li S, Lu J, Huang G, Hu K (2008) Tropical Indian Ocean basin warming and East
548 Asian summer monsoon: A multiple AGCM study. J Clim 21:6080–6088
549 Li S, Perlwitz J, Quan X, Hoerling MP (2008) Modelling the influence of North
550 Atlantic multidecadal warmth on the Indian summer rainfall. Geophys Res Lett
551 35:L05804. doi:10.1029/2007GL032901
552 Li Y, Lu R, Dong B (2007) The ENSO–Asian monsoon interaction in a coupled
553 ocean–atmosphere GCM. J Clim 20:5164–5177

554 Lu R, Dong B (2008) Response of the Asian summer monsoon to a weakening of
555 Atlantic thermohaline circulation. Adv in Atmos Sci 25:723–736
556 Lu R, Chen W, Dong B (2008) How does a weakened Atlantic thermohaline
557 circulation lead to an intensification of the ENSO−South Asian summer monsoon
558 interaction? Geophys Res Lett 35:L08706. doi: 10.1029/2008GL033394
559 Moon, JY, Wang B, Ha KJ, Lee JY (2013) Teleconnections associated with Northern
560 Hemisphere summer monsoon intraseasonal oscillation. Clim Dyn,
561 40:2761–2774
562 Ottera OH, Bentsen M, Drange H, Suo L (2010) External forcing as a metronome for
563 Atlantic multidecadal variability. Nature Geosci 3:688–694. doi:10.1038/
564 NGEO955
565 Polo I, Dong B, Sutton RT (2013) Changes in tropical Atlantic interannual variability
566 from a substantial weakening of the meridional overturning circulation. Clim Dyn
567 41: 2765–2784. doi: 10.1007/s00382-013-1716-x
568 Polo I, Rodriguez-Fonseca B, Losada T, Garcia-Serrano J (2008) Tropical Atlantic
569 variability modes (1979–2002). Part I: timeevolving SST modes related to West
570 African rainfall. J Clim 21:6457–6475. doi:10.1175/2008JCLI2607.1
571 Pope VD, Gallani ML, Rowntree PR, Stratton RA (2000) The impact of new physical
572 parameterizations in the Hadley Centre climate model: HadAM3. Clim Dyn 16:
573 123–146
574 Rayner NA, Parker DE, Horton EB, Folland CK, Alexander LV, Rowell DP, Kent EC,

575 Kaplan A (2003) Global analyses of SST, sea ice and night marine air temperature
576 since the late nineteenth century. J Geophys Res 108(D14):4407.
577 doi:10.1029/2002JD002670
578 Rodriguez-Fonseca B, Polo I, Garcia-Serrano J, Losada T, Mohino E, Mechoso CR,
579 Kucharski F (2009) Are Atlantic Niños enhancing Pacific ENSO events in recent
580 decades? Geophys Res Lett 36:L20705. doi:10.1029/2009GL040048
581 Sohn SJ, Min YM, Lee JY et al. (2012) Assessment of the long-lead probabilistic
582 prediction for the Asian summer monsoon precipitation (1983-2011) based on the
583 APCC multimodel system and a statistical model. J Geophy Res 117: D04102,
584 doi:10.1029/2011JD016308
585 Sutton RT, Hodson DLR (2007) Climate response to basin-scale warming and cooling
586 of the North Atlantic Ocean. J Clim 20:891–907
587 Svendsen, L., Kvamstø, N.G. and N. Keenlyside (2013) Weakening AMOC connects
588 Equatorial Atlantic and Pacific interannual variability, Clim Dyn doi
589 10.1007/s00382-013-1904-8
590 Timmermann A, Okumura Y, An S-I, Clement A, Dong B, Guilyardi E, Hu A,
591 Jungclaus J, Krebs U, Renold M, Stocker TF, Stouffer RJ, Sutton R, Xie S-P, Yin
592 J (2007) The influence of a weakening of the Atlantic meridional overturning
593 circulation on ENSO. J Clim 20:4899–4919
594 Tokinaga H, Xie SP (2011) Weakening of the equatorial Atlantic coldtongue over the
595 past six decades. Nat Geosci. doi:10.1038/NGEO1078

596 Wang B, Wu RG, Fu XH (2000) Pacific–East Asian teleconnection: How does ENSO
597 affect East Asian climate? J Clim 13: 1517–1536
598 Wang B, Kang IS, Lee JY (2004) Ensemble simulations of Asian-Australian monsoon
599 variability by 11 AGCMs. J Clim 17, 803–818
600 Wang B, Xiang B, Lee JY (2013) Subtropical high predictability establishes a
601 promising way for monsoon and tropical storm predictions. PNAS
602 110:2718–2722
603 Wang B, Lee JY, Xiang B (2014) Asian summer monsoon rainfall predictability: A
604 predictable mode analysis. Clim Dyn accepted
605 Wu RG, Hu ZZ, Kirtman BP (2003) Evolution of ENSO related rainfall anomalies in
606 East Asia. J Clim 16: 3742–3758
607 Xie SP (1999) A dynamic ocean-atmosphere model of the tropical Atlantic decadal
608 variability. J Clim 12:64–70
609 Xie SP, Hu K, Hafner J, Tokinaga H, Du Y, Huang G, Sampe T (2009) Indian Ocean
610 capacitor effect on Indo–Western Pacific climate during the summer following El
611 Niño. J Clim 22:730–747
612 Yang J, Liu Q, Xie SP, Liu Z, Wu L (2007) Impact of the Indian Ocean SST basin
613 mode on the Asian summer monsoon. Geophys Res Lett 34:L02708.
614 doi:10.1029/2006GL028571
615 Yu K, Xie SP, Lau NC, Vecchi GA (2013) Origin of seasonal predictability for
616 summer climate over the Northwestern Pacific. PNAS 110:7574–7579

617 Yun, KS., Ha KJ, Wang B (2010) Impacts of tropical ocean warming on East Asian
618 summer climate. Geophys Res Lett 37:L20809
619 Yun, KS, Yeh SW, Ha KJ (2013) Distinct impact of tropical SSTs on summer North
620 Pacific high and western North Pacific subtropical high. J Geophys Res
621 118:4107–4116
622 Zhai X, Sheldon L (2012) On the North Atlantic ocean heat content change between
623 1955–1970 and 1980–1995. J Clim 25:3619–3628.
624 doi:10.1175/JCLI-D-11-00187.1
625 Zhang R, Delworth TL (2005) Simulated tropical response to a substantial weakening
626 of the Atlantic thermohaline circulation. J Clim 18:1853–1860
627 Zhang R, Delworth TL et al (2013) Have Aerosols Caused the Observed Atlantic
628 Multidecadal Variability? J Atmos Sci 70:1135–1144. doi:
629 http://dx.doi.org/10.1175/JAS-D-12-0331.1
630

631

632 **Captions**

633 **Table 1.** Correlation coefficients among the indices in observations. The tropical
634 North Atlantic (TNA), Niño 4, Niño 3, North Indian Ocean (NIO), western North
635 Pacific (WNP) and the western North Pacific anticyclonic anomaly (WNPAC) indices
636 are defined as the anomalies averaged over the region (0°−20°N, 30°−80°W),
637 (5°S−5°N, 160°E−150°W), (5°S−5°N, 90°−150°W), (5°−20°N, 40°−100°E), (5−25°N,
638 110°−160°E) and (0°−25°N, 110°−145°E), respectively. The bold ones represent that
639 the partial correlation coefficients by removing the impacts of Niño 4 index. One or
640 two asterisks represent the correlation coefficients are significant at 95% or 99%
641 confidence levels, respectively.

642 **Fig. 1.** Regression of normalized boreal summer months (JJA)-mean SST anomalies
643 onto the WNPAC index in observations. (a) Original SST anomalies. (b) SST
644 anomalies after removing the impact of Niño 4 SST. The regions within the black
645 lines indicate where the anomalies are significant at 95% confidence level by F-test.
646 The dashed rectangles represent the regions to define the indices.

647 **Fig. 2.** Time series for the TNA (°C) and WNPAC (10^6 m^2 s^{-1}) indices for original data
648 (a) and after eliminating the Niño 4 SST (b) from 1967 to 1997 in observations.

649 **Fig. 3.** Lead-lag correlation coefficients between monthly-mean TNA and JJA-mean
650 WNPAC indices from 1967 to 1997 in observations. Zero month (-1 month) means

July (June) and left-hand (right-hand) side indicate TNA (WNPAC) leading. Black and red lines represent the lead-lag correlation by original data and after eliminating Niño 4 SST impact, respectively. The dark dashed line represents the 95% confidence level by t-test.

Fig. 4. Same as Fig. 1, but for the 160 years simulation of the CNTL.

Fig. 5. Differences of climatological mean SST (°C; a), interannual standard deviation of SST anomalies (°C; b) and interannual standard deviation of SST anomalies after removing the Niño 4 index (°C; c) in JJA between the 1Sv and the CNTL. The regions within the black lines indicate where the differences are significant at 95% confidence level by *t*-test.

Fig. 6. Regression of 850-hPa stream function anomalies (10^6 m^2 s^{-1}) onto the TNA index in the CNTL (a) and the 1Sv (b).

Fig. 7. Same as Fig. 6, but for the 200-hPa velocity potential anomalies (10^6 m^2 s^{-1}).

Fig. 8. Same as Fig. 6, but for the precipitation anomalies (mm day^{-1}) and 850-hPa wind anomalies. For 850-hPa wind, only the anomalies are significant at 95% confidence level by F-test are shown.

Fig. 9. Same as Fig. 6, but for the SST anomalies (°C).

Fig. 10. Differences of climatological mean depth of 20°C thermocline (D20; m) in JJA between the 1Sv and the CNTL. The regions within the black lines indicate where the differences are significant at 95% confidence level by *t*-test. The dashed rectangle represents the region to calculate the difference of D20.

672 **Fig. 11.** Same as Fig. 6, but for the 850-hPa stream-function anomalies (10^6 m^2 s^{-1}; left
673 panel) and 200-hPa velocity potential anomalies (10^6 m^2 s^{-1}; right panel) during the
674 negate phase of AMO (a, c) and the positive phase of AMO (b, d) in observations.

Table 1. Correlation coefficients among the indices in observations. The tropical North Atlantic (TNA), Niño 4, Niño 3, North Indian Ocean (NIO), western North Pacific (WNP) and the western North Pacific anticyclonic anomaly (WNPAC) indices are defined as the anomalies averaged over the region (0°−20°N, 30°−80°W), (5°S−5°N, 160°E−150°W), (5°S−5°N, 90°−150°W), (5°−20°N, 40°−100°E), (5−25°N, 110°−160°E) and (0°−25°N, 110°−145°E), respectively. The bold ones represent that the partial correlation coefficients by removing the impacts of Niño 4 index. One or two asterisks represent the correlation coefficients are significant at 95% or 99% confidence levels, respectively.

	TNA	Niño 4	Niño 3	NIO	WNP
WNPAC	0.344	-0.375*	-0.374*	0.194	0.316
Niño 4	0.281	1.000	0.657**	0.417*	0.131
WNPAC (-Niño 4)	**0.506****	**/**	**-0.183**	**0.415***	**0.398***

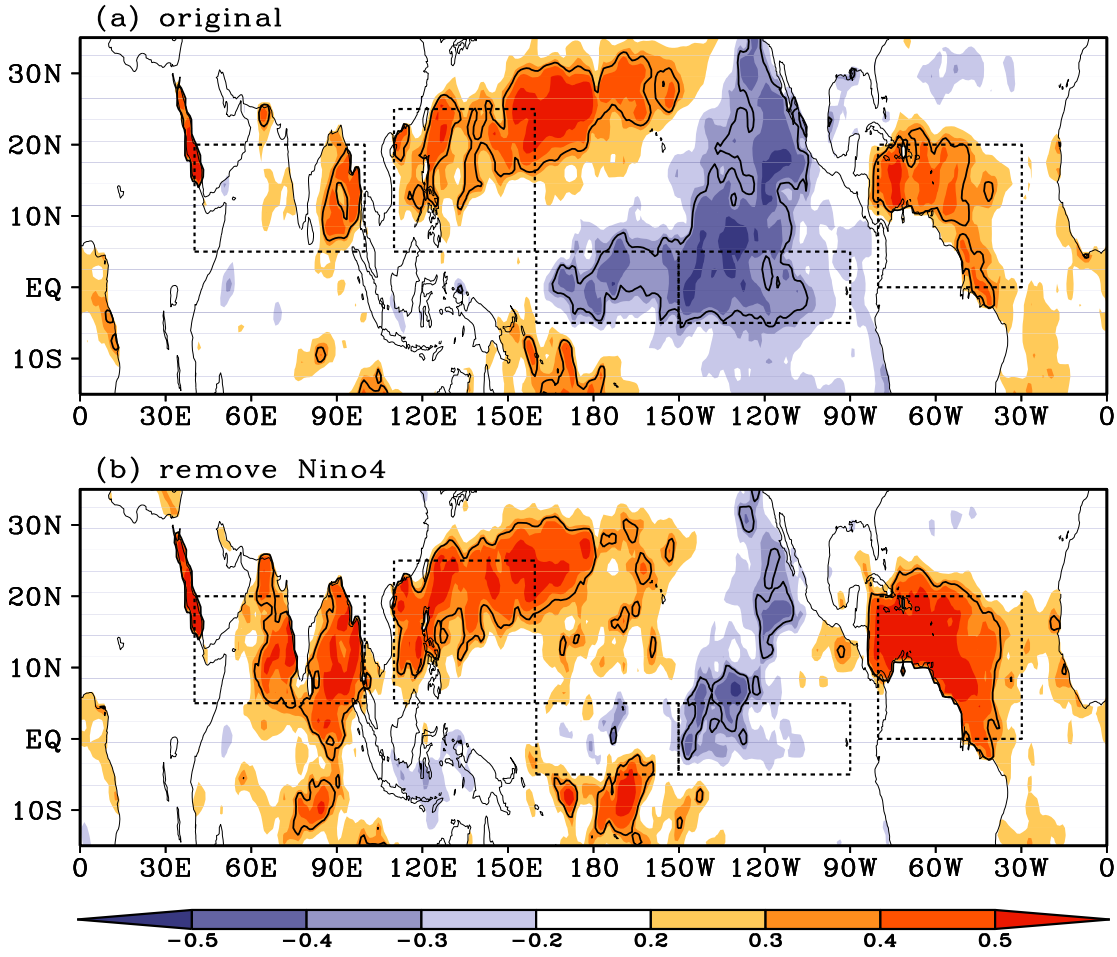

Fig. 1. Regression of normalized boreal summer months (JJA)-mean SST anomalies onto the WNPAC index in observations. (a) Original SST anomalies. (b) SST anomalies after removing the impact of Niño 4 SST. The regions within the black lines indicate where the anomalies are significant at 95% confidence level by F-test. The dashed rectangles represent the regions to define the indices.

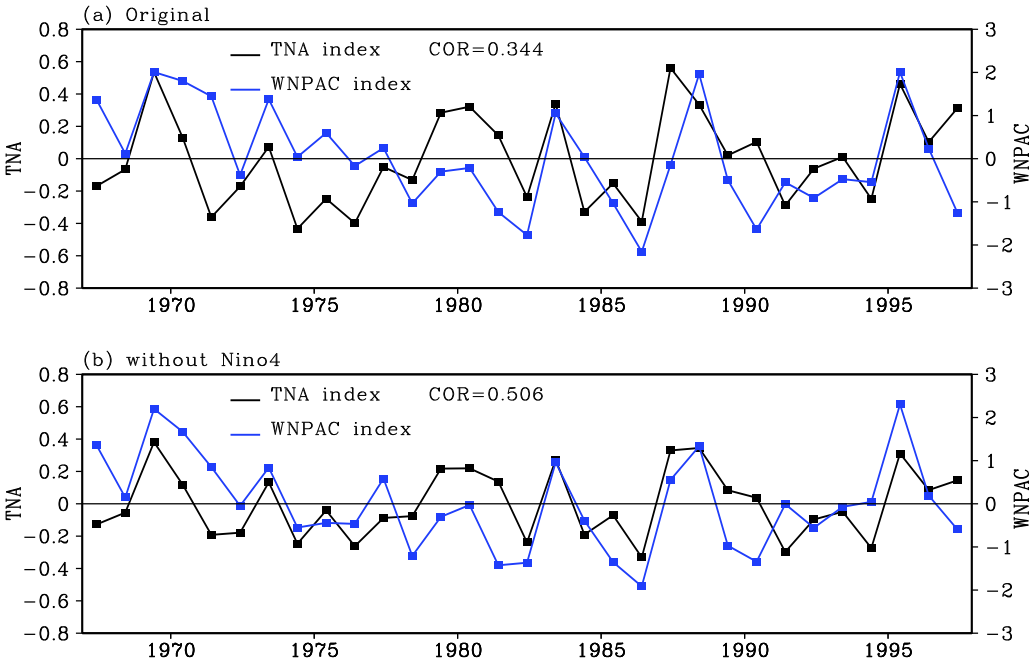

Fig. 2. Times series for the TNA (°C) and WNPAC (10^6 m^2 s^{-1}) indices for original data (a) and after eliminating the Niño 4 SST (b) from 1967 to 1997 in observations.

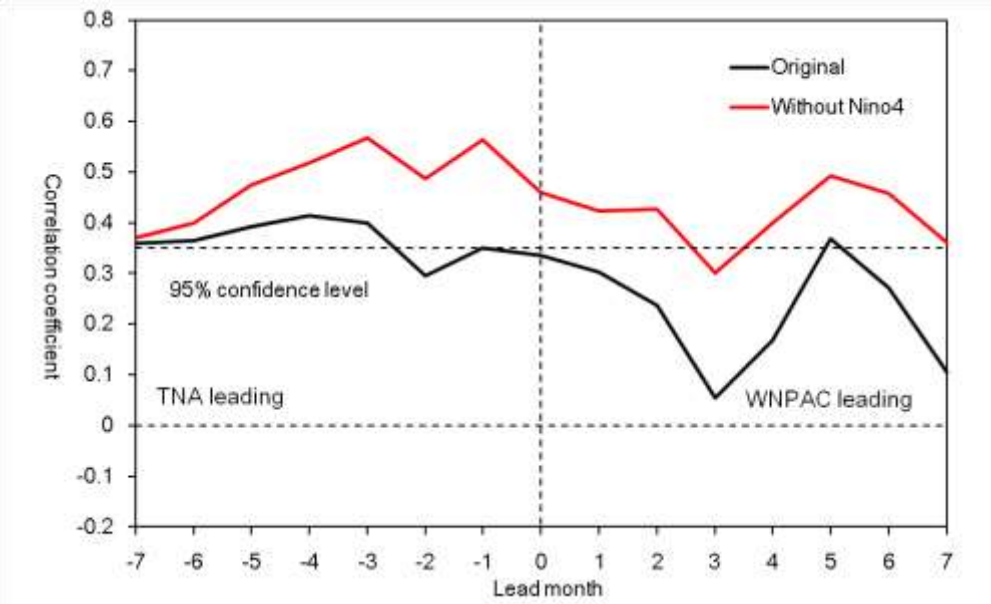

Fig. 3. Lead-lag correlation coefficients between monthly-mean TNA and JJA-mean WNPAC indices from 1967 to 1997 in observations. Zero month (-1 month) means July (June) and left-hand (right-hand) side indicate TNA (WNPAC) leading. Black and red lines represent the lead-lag correlation by original data and after eliminating Niño 4 SST impact, respectively. The dark dashed line represents the 95% confidence level by t-test.

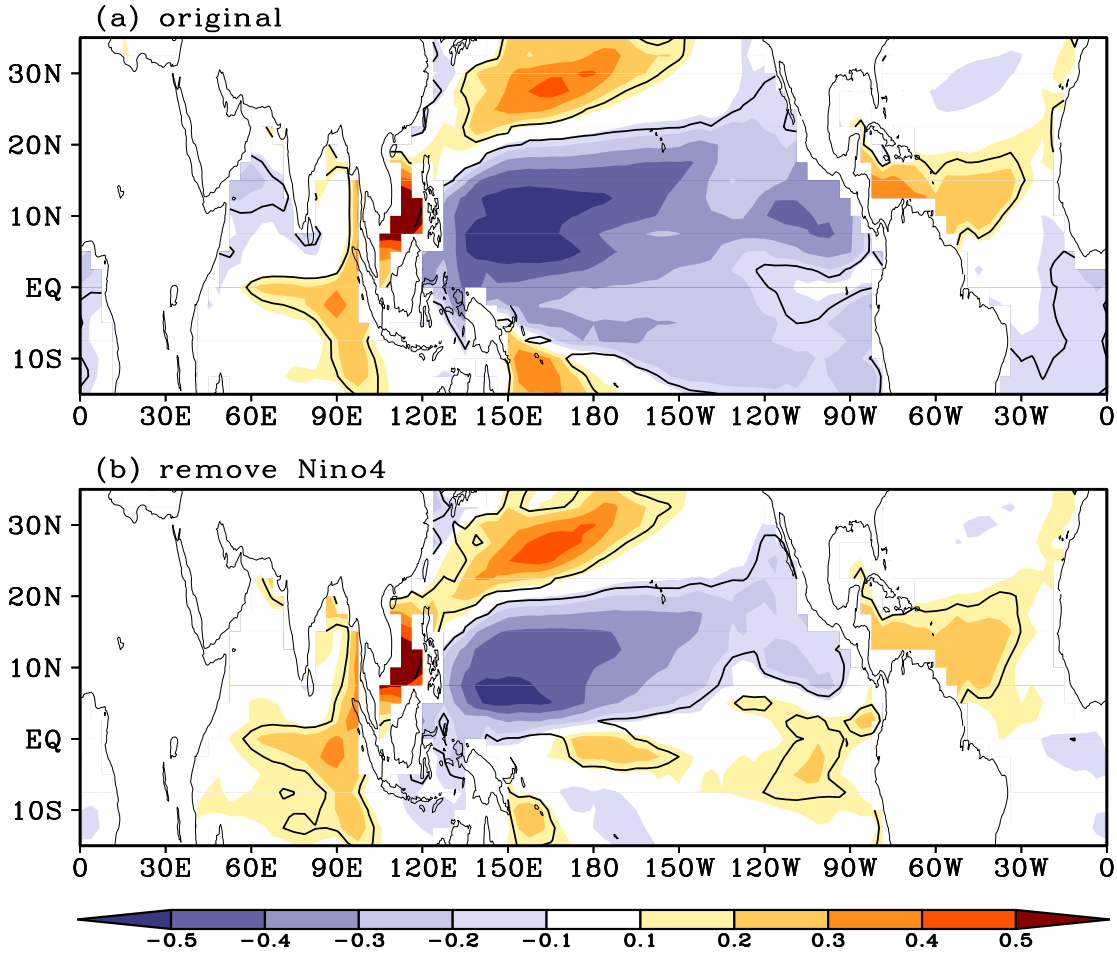

Fig. 4. Same as Fig. 1, but for the 160 years simulation of the CNTL.

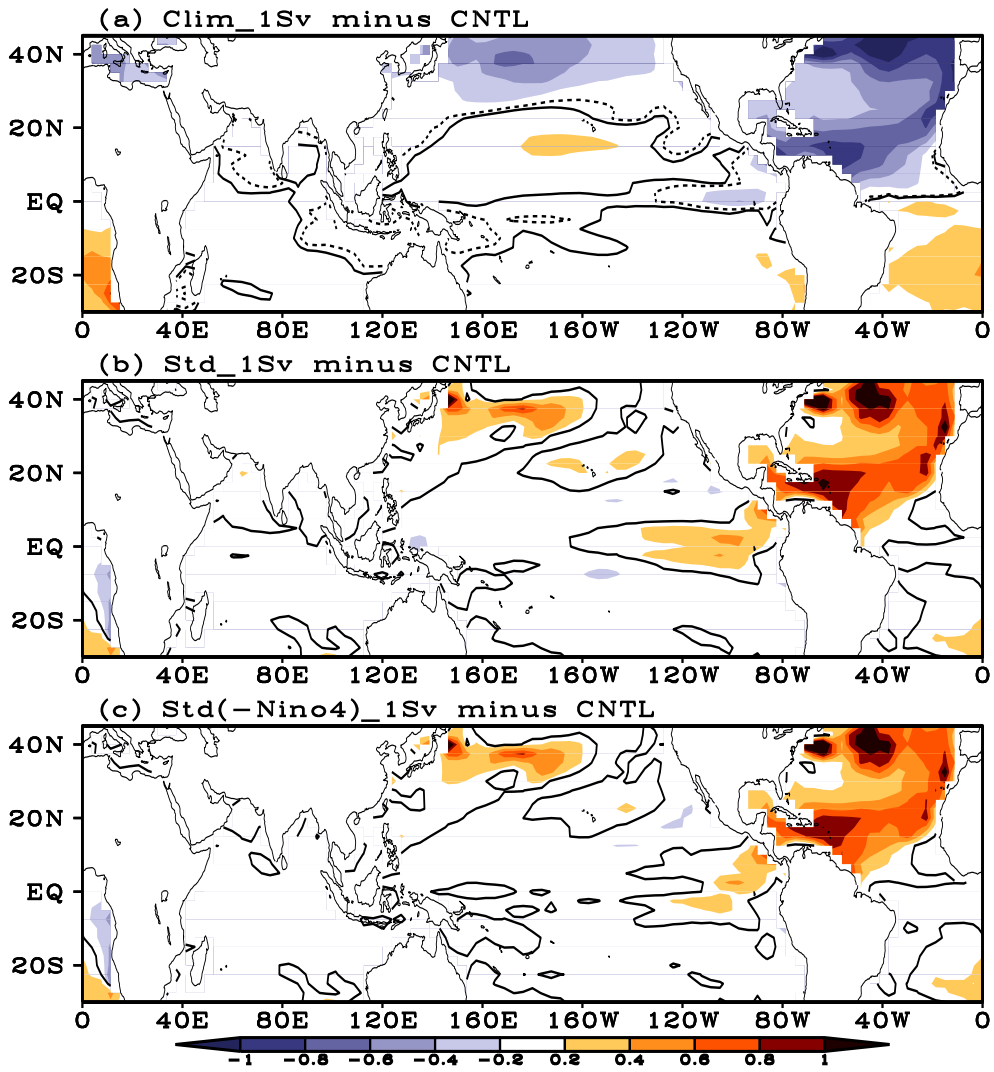

Fig. 5. Differences of climatological mean SST (°C; a), interannual standard deviation of SST anomalies (°C; b) and interannual standard deviation of SST anomalies after removing the Niño 4 index (°C; c) in JJA between the 1Sv and the CNTL. The regions within the black lines indicate where the differences are significant at 95% confidence level by *t*-test.

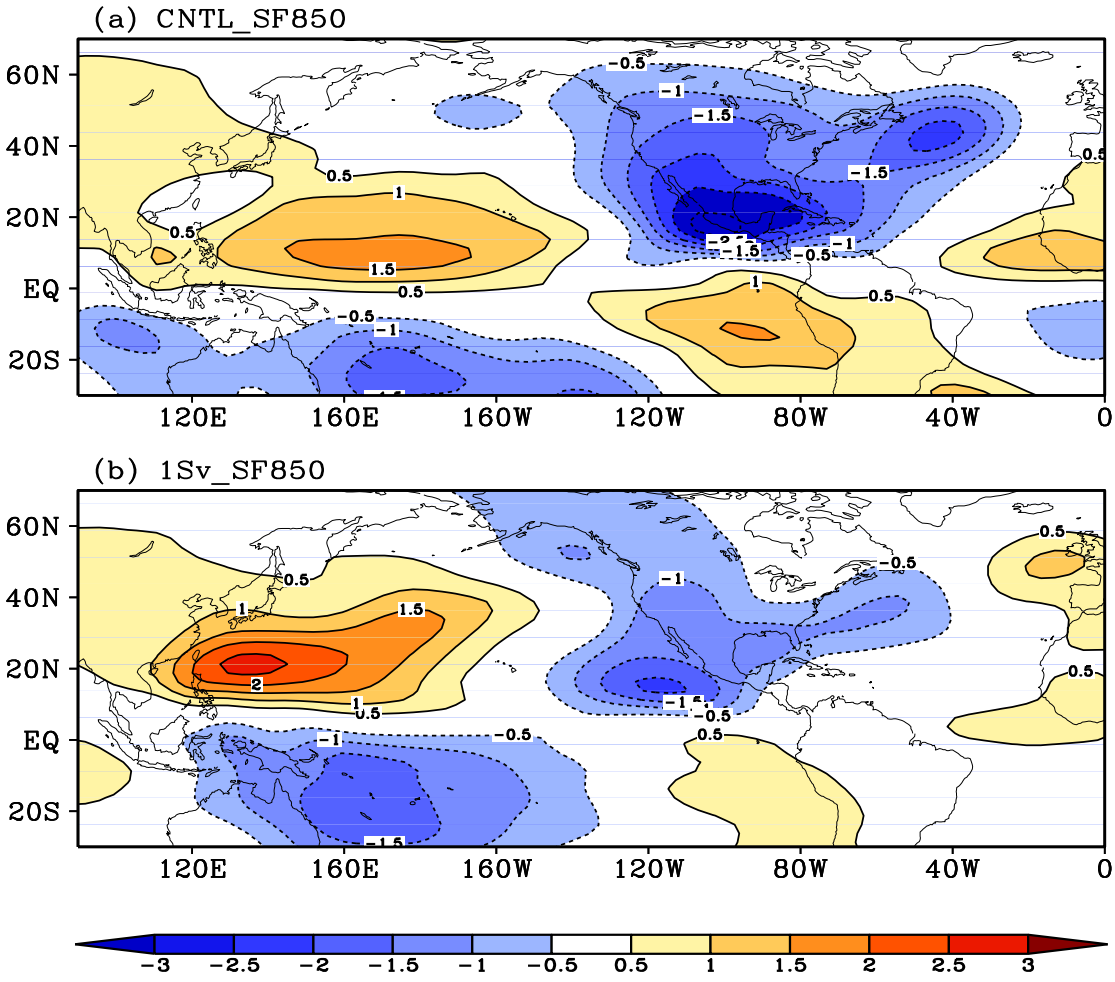

Fig. 6. Regression of 850-hPa stream function anomalies (10^6 m^2 s^{-1}) onto the TNA index in the CNTL (a) and the 1Sv (b).

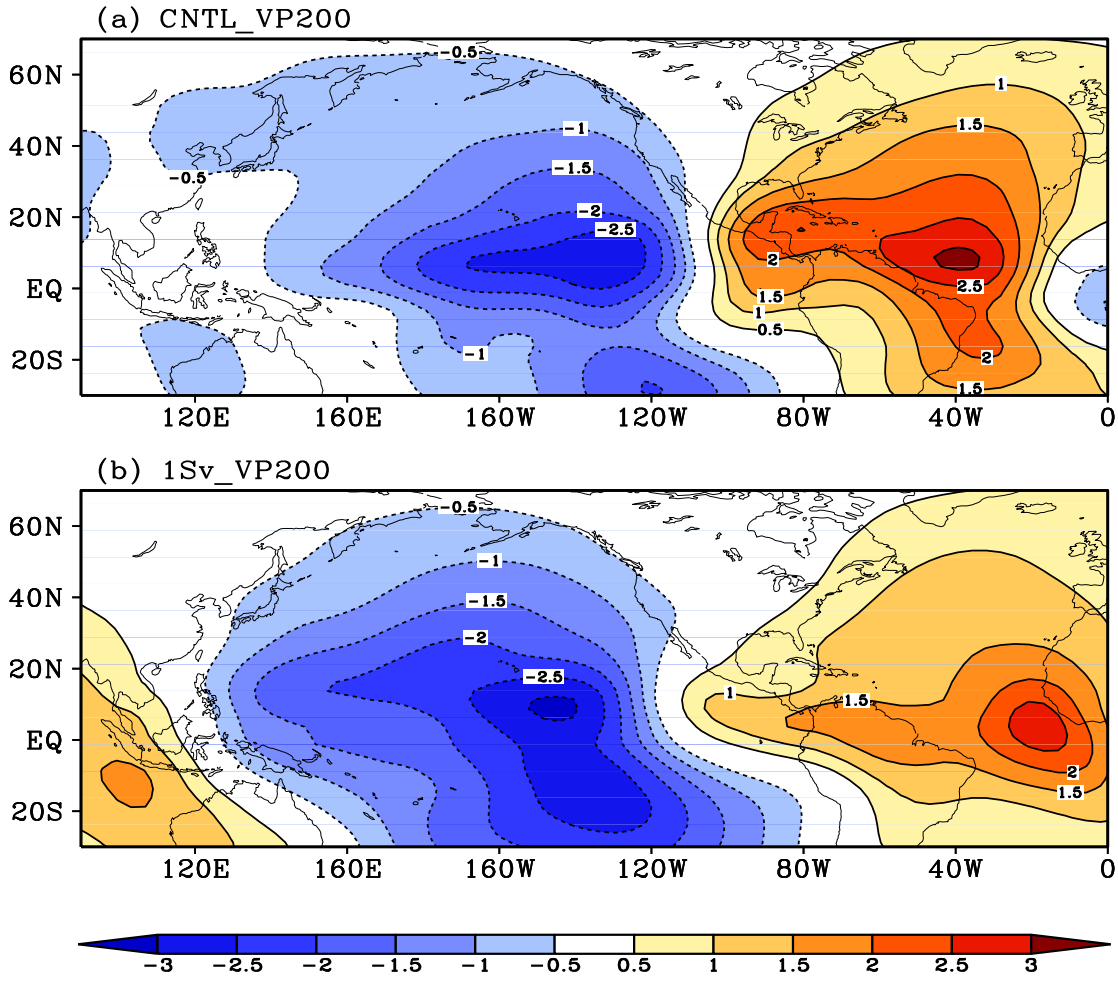

Fig. 7. Same as Fig. 6, but for the 200-hPa velocity potential anomalies (10^6 m^2 s^{-1}).

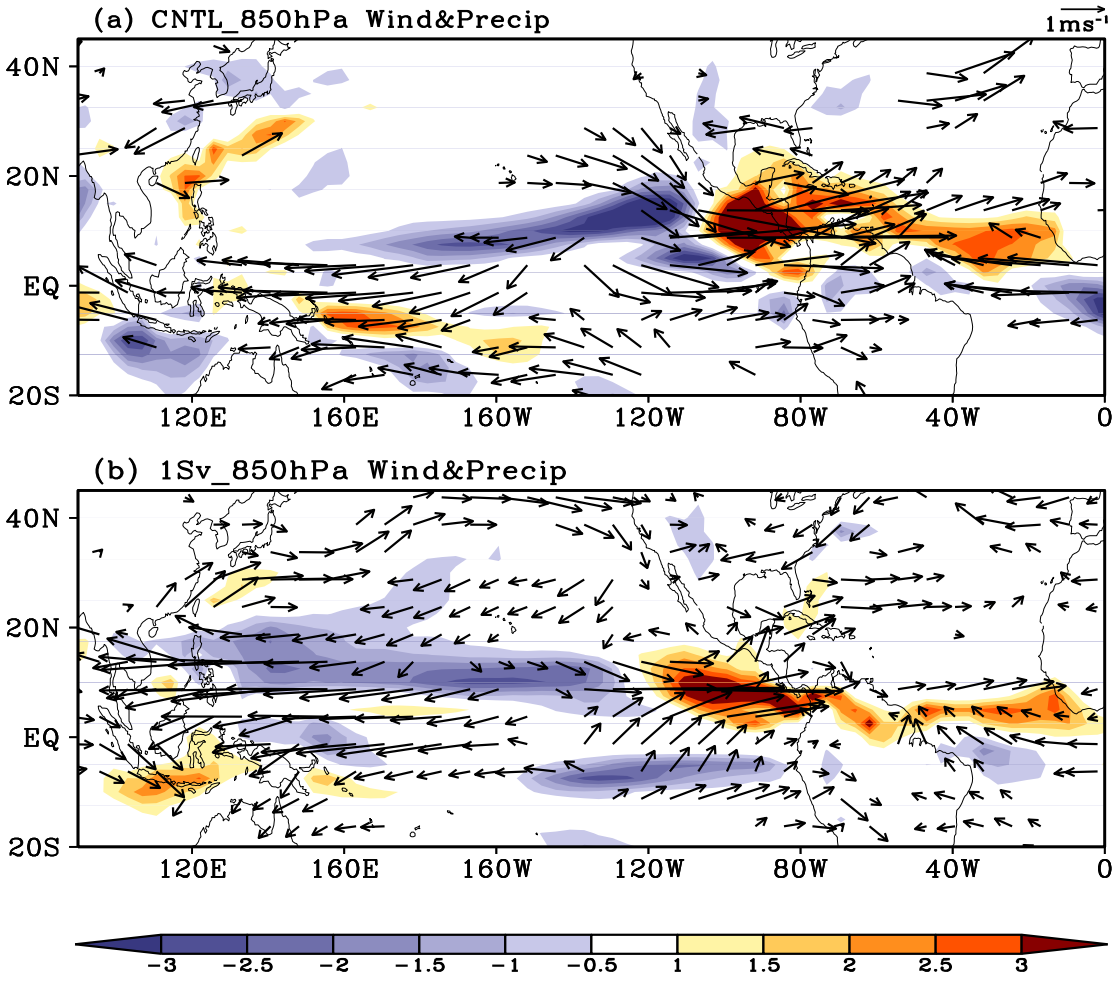

Fig. 8. Same as Fig. 6, but for the precipitation anomalies (mm day^{-1}) and 850-hPa wind anomalies. For 850-hPa wind, only the anomalies are significant at 95% confidence level by F-test are shown.

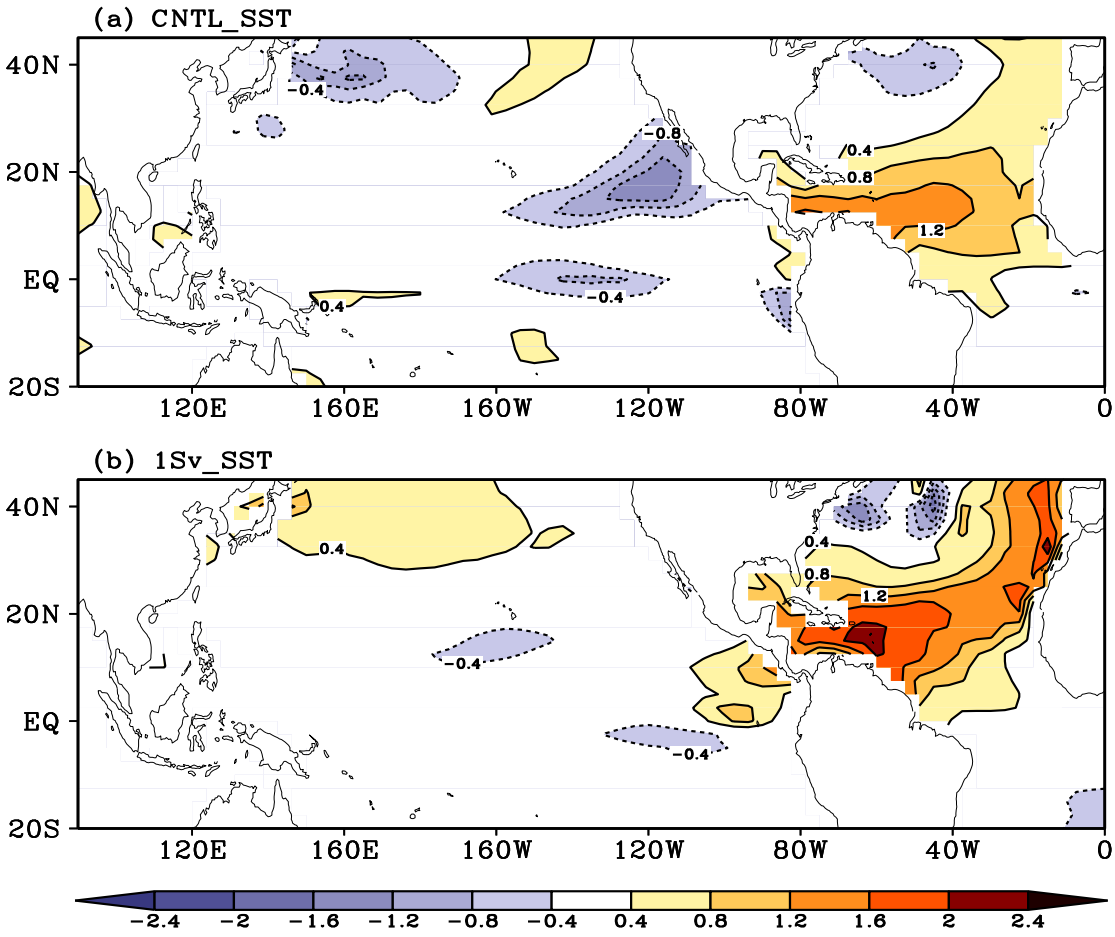

Fig. 9. Same as Fig. 6, but for the SST anomalies (°C).

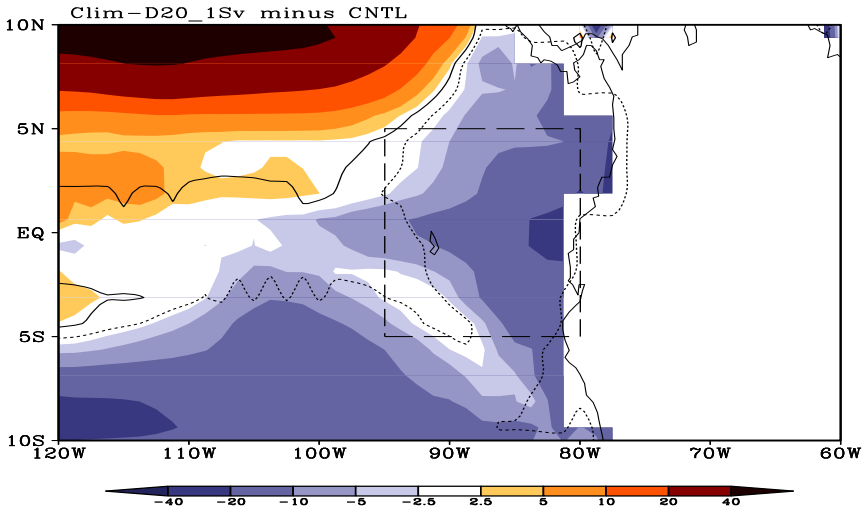

Fig. 10. Differences of climatological mean depth of 20°C thermocline (D20; m) in JJA between the 1Sv and the CNTL. The regions within the black lines indicate where the differences are significant at 95% confidence level by *t*-test. The dashed rectangle represents the region to calculate the difference of D20.

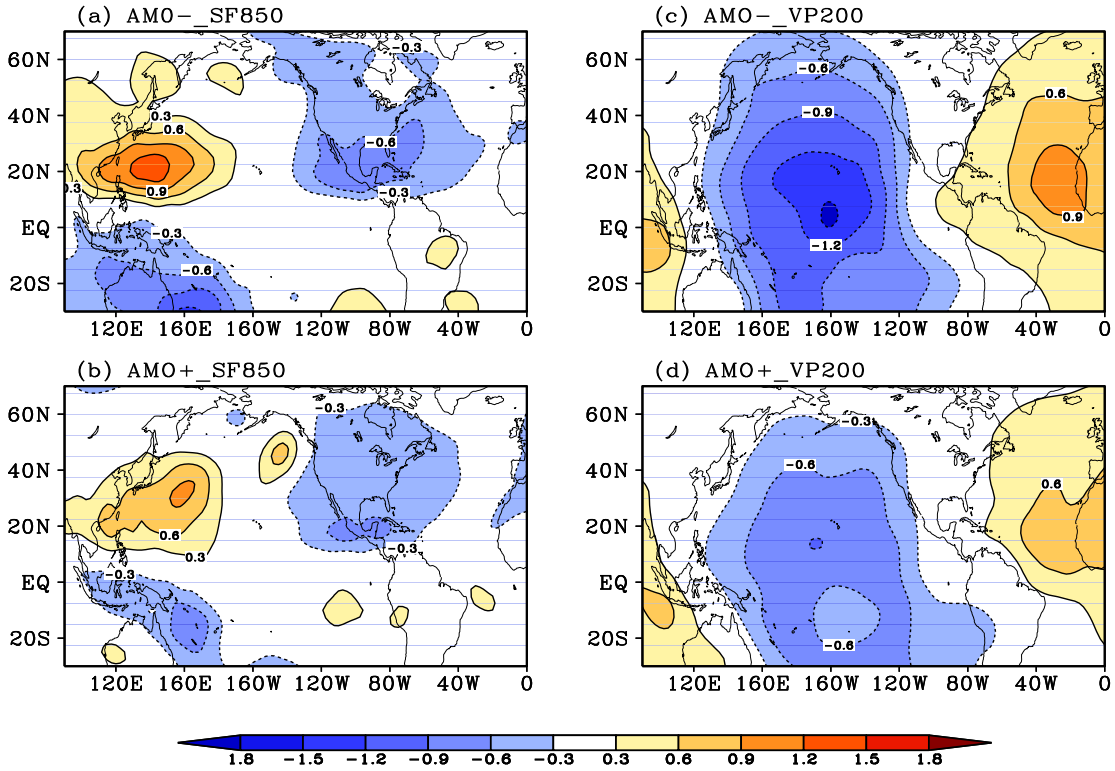

Fig. 11. Same as Fig. 6, but for the 850-hPa stream-function anomalies (10^6 m^2 s^{-1}; left panel) and 200-hPa velocity potential anomalies (10^6 m^2 s^{-1}; right panel) during the negative phase of AMO (a, c) and the positive phase of AMO (b, d) in observations.